Iranian Journal of Materials Forming 8 (3) (2021) 26-33

Online ISSN: 2383-0042

IJMF

Iranian Journal of Materials Forming

Journal Homepage: http://ijmf.shirazu.ac.ir

Research Article

Synthesis and Consolidation of Ag/ZnO Composite Powders via SPS Method

M. Ardestani*

Department of Materials Engineering, Science and Research Branch, Islamic Azad University, Tehran, Iran

ARTICLE INFO

Article history:

Received 25 May 2021
Reviewed 5 June 2021
Revised 15 June 2021
Accepted 29 June 2021

Keywords:

Silver matrix composites
Consolidation
Composite
Spark plasma sintering

ABSTRACT

The present research was conducted to synthesize and densify Ag/8wt.% ZnO composites via co-precipitation and spark plasma sintering (SPS) methods. The initial precipitates were precipitated by adding ammonium hydrogen carbonate solution to a solution mixture of silver and zinc nitrate. The precipitates were characterized by using the particle size analyzer and X-ray diffraction techniques. The precipitates were calcined at 500°C and consolidated with SPS method for 5 and 10 min at 540°C under 35 MPa in vacuum. The results showed that rearrangement and bulk deformation had a significant effect on densification of the composite powders. The scanning electron microscopy investigations revealed that the SPSed composites had nearly dense microstructures with homogenous and fine dispersion of ZnO particles within the silver matrix. Moreover, it was confirmed that prolonging the sintering time from 5 to 10 min had no significant effect on the microstructure, relative density and hardness of the samples. Composites with relative densities above 99% and 62 HV hardness were synthesized through the applied procedure.

1. Introduction

Metal Matrix Composites (MMCs) are a group of materials used for fabrication of various industrial components in areas such as, transportation, electronics, aerospace, as well as automotive and electric power transmission [1-3]. Silver and copper are the most frequently utilized metals as the matrix phase in the composites used in producing electrical components like relays and switches. In such kinds of composites different compounds such as oxides and carbides are used as the second phase or, in other words, the reinforcement. Generally, the compounds and metals like WC, ZnO, CuO and W are applied-in particle form-as the reinforcement in these kinds of composites [4-7].

Silver reinforced zinc oxide MMCs are one of the materials categorized in the above-mentioned composites. Ag/ZnO composites are mainly employed in fabricating low-voltage circuit breakers related to 200A. Different reinforcements are used as the second phase in the silver matrix composites utilized to produce circuit breakers. However, according to the working conditions of the breaker, the reinforcement may vary. Ag/ZnO composites are generally fabricated via a powder metallurgy process that includes pressing and sintering of Ag/ZnO powder mixtures.

* Corresponding author
E-mail address: m-ardestani@srbiau.ac.ir (M. Ardestani)
https://doi.org/10.22099/ijmf.2021.40783.1184

Nonetheless, for further densification, the sintered composite is repressed and annealed after sintering [7] which could be a time-consuming process. Over the recent years, much research has been conducted on the synthesis of Ag/ZnO composites to produce composites with homogenous dispersion of ZnO within the silver matrix with desired properties. These studies have mainly focused on the synthesis of Ag/ZnO composite powders with high sinterability. It has been shown that owing to high sinterability of the composite powders, the sintered composites need not to be more densified via secondary densification processes such as extrusion or cold pressing. Mechanical milling, mechanochemical, hydrothermal and chemical routes are some of the numerous applied techniques for the synthesis of Ag/ZnO composite powders [8-12]. Moreover, various sintering processes like hot pressing have been applied for densification of Ag/ZnO composite powders [13]. Meanwhile, SPS of Ag/ZnO composite powders has not been investigated yet. SPS, which is known as plasma activated sintering (PAS), is a short time densification method which has been applied for consolidation of metallic, ceramic, and composite powders in relatively low temperatures [14-17]. Ray et al. investigated the sintering of Ag/WC composites. They confirmed that SPS composites were more homogeneous, tougher, and softer than conventionally processed equivalents [18]. Li et al. studied the arc erosion characteristics of Ag/8 wt.% Ni composites prepared with powder metallurgy and SPS techniques [19]. It was shown that the bounce height significantly influences the arc parameters. Sayyad et al. investigated the SPS of Ag/reduced graphene oxide reinforced copper matrix composites [20]. They reported that by adding 0.8 vol% of Ag/rGO, the bending strength of SPSed samples increased 187 MPa in comparison to pure Cu.

In this research, the synthesis and densification of Ag/ZnO composite powders was investigated via co-precipitation and SPS methods. Furthermore, the microstructure and properties of the synthesized powders and the sintered samples were evaluated.

2. Experimental Method

Silver nitrate (IRAN SHIMI, $AgNO_3$, 99.99% purity), zinc nitrate (IRAN SHIMI, Zn $(NO_3)_2.6H_2O$, 99.9% purity) and ammonium hydrogen carbonate (Merck, NH_4HCO_3, >99% purity) were utilized as the precursors. In order to synthesize Ag/8 wt.% ZnO composites, a mixture of silver and zinc nitrate solutions were made in distilled water. Additionally, ammonium hydrogen carbonate solution (1 M) was added to the mixture dropwise. The particle size distribution of the precipitates was determined using a particle size analyzer. The precipitates were calcined at 500°C in air atmosphere. Phase identification of the precipitates and calcined powders was carried out with X-ray diffraction (XRD) method using Cu-K_α radiation (λ = 1.5406 Å). The calcined powders were consolidated via spark plasma sintering (SPS) method at 540°C for 5 and 10 min in vacuum under 35 MPa. The microstructure of the powders and sintered samples were evaluated through field emission scanning electron microscopy (FESEM; MIRA3, TESCAN) equipped with energy dispersive spectroscopy (EDS). The density of the sintered composites was determined according to the Archimedes principle. The relative density of the sintered samples was determined by dividing the measured density to the theoretical one (9.81 g/cm^3). The Vickers hardness of the samples was measured by a Vickers hardness tester under 10 kgf load and a load time of 15 s. The hardness of the composites was determined by estimating the average of at least three hardness measurements.

3. Results and Discussion

Fig. 1 represents the result of particle size analysis of the initial precipitates. The D10, D50 and D90 values were 2.42, 7.66 and 14.1 µm, respectively. Furthermore, the volume statistics parameter, in other words the mean, median, and mode, were respectively 8.06, 7.66, and 9.56 µm. According to the results, the size of the particles ranged from 1 to 23 µm. Fig. 2 depicts the morphology of the initial precipitates in different magnifications. According to this figure, the precipitates

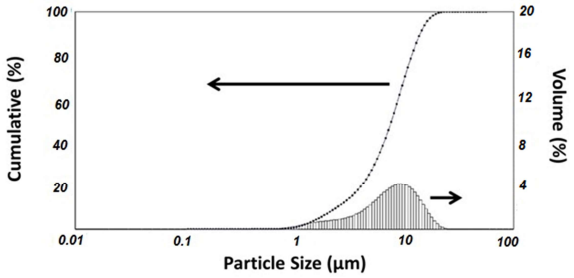

Fig. 1. The particle size distribution of the initial precipitates.

represented two main morphologies: namely nano-flower and polygonal. The thickness of the sheet-like features in the microstructure of the nano-flower regions was lower than 100 nm (Fig. 2(c)). Furthermore, the sheets had similar thickness all over the microstructure. On the basis of the EDS analysis result, which is shown in Fig. 2(d) and (e), the nano-flower particles mainly consisted of Ag while the polygonal ones were composed of both Ag and Zn compounds.

The XRD pattern of the precipitates is demonstrated in Fig. 3(a). According to the pattern, the initial precipitates contained Ag_2CO_3 and $ZnCO_3$, that is similar to the result of the previous study in which another precursor ($(NH_4)_2CO_3$) was used [21]. In the previous research, the silver and zinc carbonates were precipitated from two separate silver and zinc nitrate solutions in water and then by mixing the solutions, the desired Ag/Zn containing precipitates were obtained. However, the morphology of the precipitates herein completely differed from those in the previous research. According to the FESEM and XRD results, it seems that in the regions containing Ag and Zn compounds (the polygonal particles), either silver or zinc carbonate was primarily formed, and it then acted as a nucleation site for the other one. This phenomenon contributes to an appropriate distribution of the constituents, which could be one of the advantages of the applied precipitation method. Fig. 3(b) illustrates the XRD pattern of the calcined precipitates at 500°C. As illustrated, the calcined precipitates contain Ag and ZnO implying the complete calcination of the precipitates to the desired constituents.

Fig. 4 shows the FESEM micrograph of the calcined precipitates. As could be seen, the morphology of the calcined powders is not similar to the initial precipitate due to thermal decomposition of the carbonates and

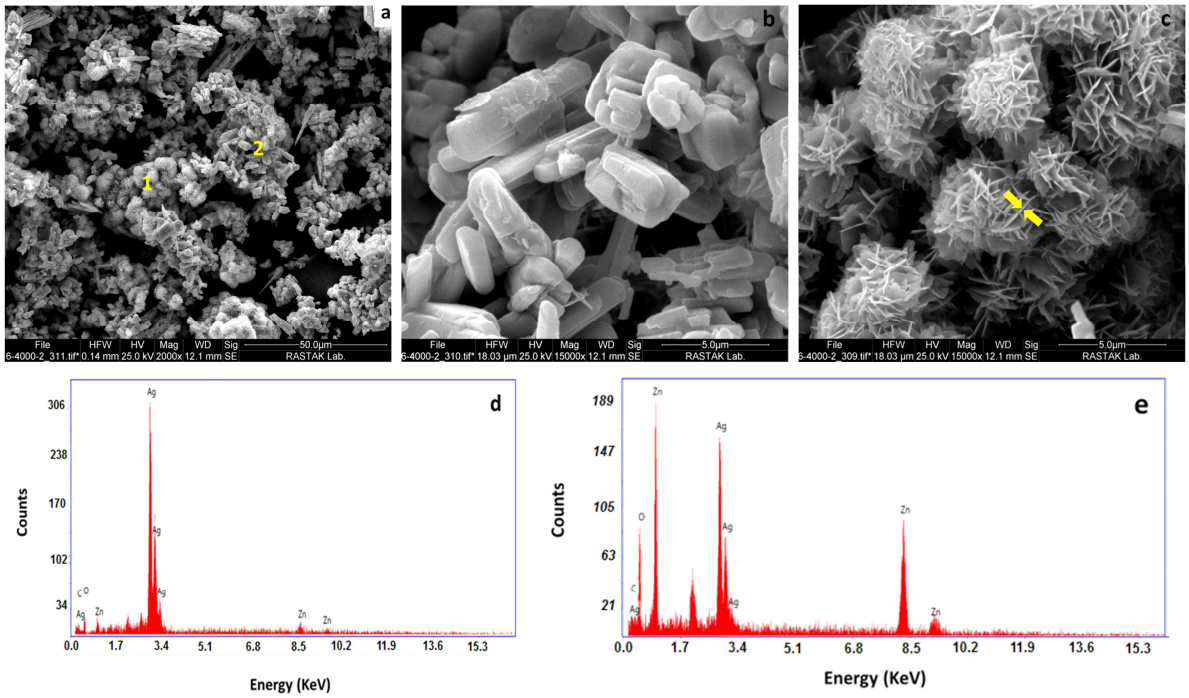

Fig 2. (a) FESEM micrograph of the initial precipitates. (b) Polygonal and (c) Nano-flower morphologies. The arrows show the thickness of the sheet-like features. (d) EDS analysis of points 1 in (a). (e) EDS analysis of points 2 in (a).

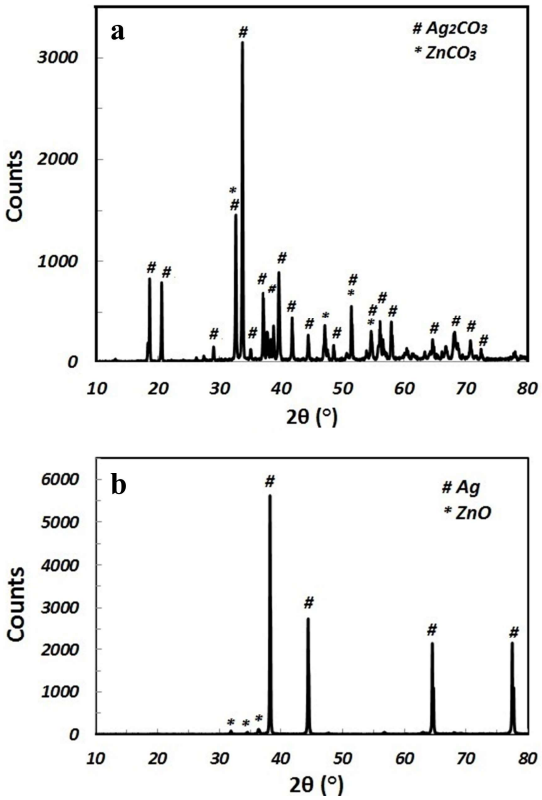

Fig. 3. XRD pattern of (a) The initial precipitates. (b) The calcined precipitates.

evaporation of carbon dioxide and water. In addition, neck-like regions could be seen within the microstructure of the calcined powders which confirms the solid-state reaction of the powder particles during calcination (Fig. 4(d)). The driving force of necking is the reduction in the free surface of the powder particles and the decrease in the superficial energy [22]. Fig. 4(c) represents the EDS analysis results of the neck-like regions. Formation of the silver-containing neck-like regions is due to atomic diffusion of Ag at relatively low temperatures [23].

Fig. 5(a) and (b) show the punch displacement and displacement rate as a function of temperature during SPS of the composite powders. As shown, the curve of displacement versus temperature shows three distinct regions (I, II, III) with different slopes corresponding to different stages of densification. Additionally, the displacement rate versus temperature curve indicated three peaks: a sharp one at about 55°C, a weak one at 140°C, and the third one at 515°C. The three above-

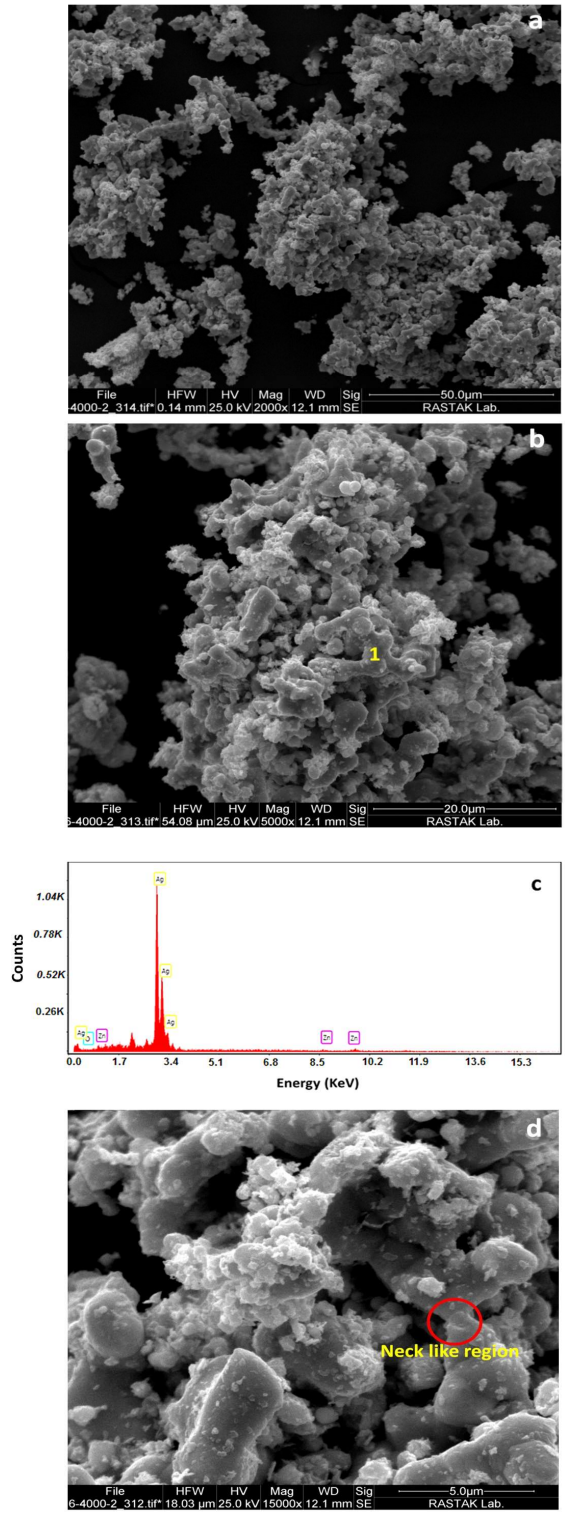

Fig. 4. (a and b) FESEM micrograph of the calcined precipitates in different magnifications. (c) EDS analysis of point 1 in (b). (d) Formation of neck like regions in the microstructure of the calcined powders.

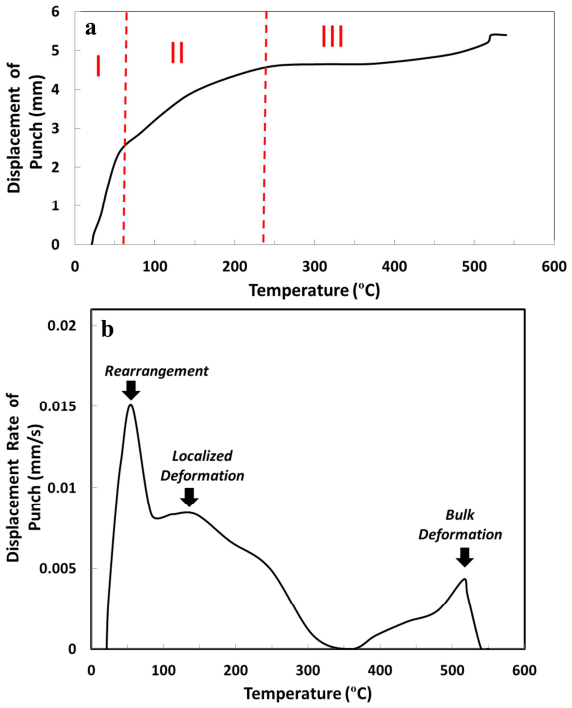

Fig. 5. (a) Punch displacement, and (b) Punch displacement rate as a function of temperature during SPS of Ag/ZnO composite powders under 35 MPa.

mentioned peaks were attributed to the rearrangement of powder particles, localized, and bulk deformation, respectively [14, 24-26]. However, at higher temperatures at the last stage of SPS, the mass transport phenomena occurred and is responsible for extensive sintering. Given the obtained results, it could be concluded that the rearrangement stage had a significant effect on densification of powder particles during SPS, which is due to the existence of particles with different sizes within the microstructure of the precipitates (Fig. 1) Generally, the powder particles with a relatively wider size range show better compressibility than the other ones at the rearrangement stage due to filling the free spaces between the bigger powder particles with the little ones. Furthermore, the breakage of the agglomerates at the rearrangement stage improves the densification of the powder particles. The rearrangement of powder particles is one of the densification mechanisms in other consolidation processes like hot press [14, 24-26]. In general, once the particle size range is wide, this mechanism could be more effective during densification process (according to Fig. 1, the size of the particles ranged from 1 to 23 µm). This is due to filling the porosities between the large particles with the smaller ones. The slope of the punch displacement versus temperature in Fig. 5(a) reveals the effect of rearranging the powder particles on densification during the consolidation process at low temperatures. However, as known, in order to obtain a nearly dense microstructure through hot press, a relatively long sintering time is needed. Thus, it could be concluded that other than rearrangement, other mechanisms, owing to the formation of plasma between the powder particles, have a significant effect on densification of powder particles in a relatively short time during SPS. During SPS, the temperature rises to above 1000ºC within a very short time under pulse energized and pressure which results in the fabrication of sintered compacts with high relative density. The effectivity of the SPS method is due to the homogenous distribution of the heat over the entire volume of the powder compact at microscopic scale and dissipation of heat at the contact point of the powder particles where the energy is required for sintering [14, 24].

Fig. 6 exhibits the FESEM micrograph of the sintered samples at 540°C with 5, and 10 min remaining time at sintering temperature at the backscattered (BSE) mode. The micrographs show a nearly dense microstructure of the sintered samples. No detectable differences could be observed between the microstructure of the two groups of the samples with 5 and 10 remaining times at the sintering temperature, which implies that sintering of the samples for 5 min led to the dense microstructure and there is no need to prolong the sintering time to 10 min. Moreover, the relative density of both samples was above 99% which is in good agreement with the microscopic investigations. The extremely low time needed for densification in the SPS process confirms the superiority of SPS process to other densification processes such as conventional sintering and hot press [27].

A typical elemental map analysis of Ag and Zn of the sintered composites is demonstrated in Fig. 7. The analysis results confirmed the fine dispersion of the ZnO particles within the Ag matrix. The mean hardness of

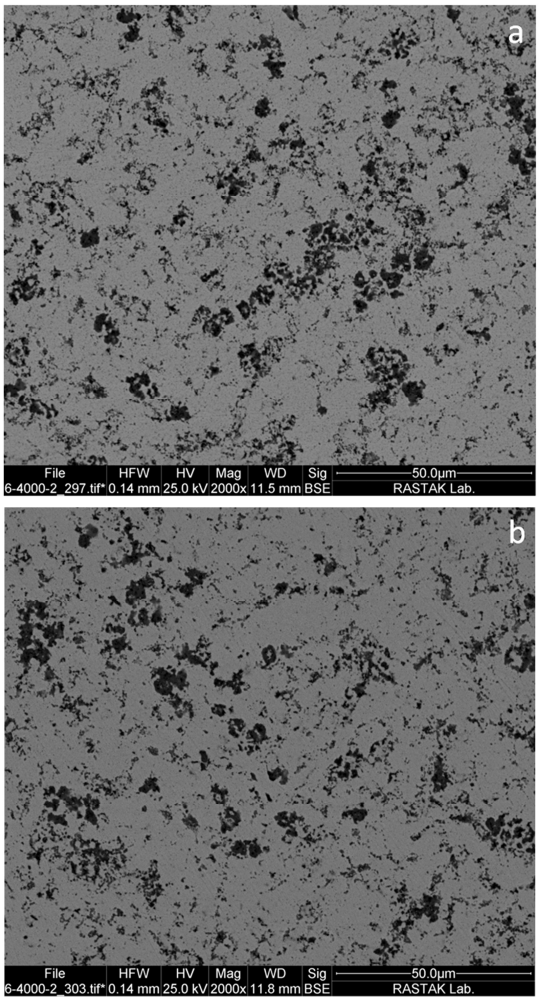

Fig. 6. FESEM (BSE mode) micrograph of the sintered composites with (a) 5 min (b) 10 min sintering times.

both groups of the sintered samples was 62 HV which is about 35 HV higher than that of pure silver. This shows the effective role of ZnO in improving the mechanical properties and, more importantly, the hardness of the composite as the reinforcement (the hardness of pure silver is 27 HV). Furthermore, the difference in the thermal expansion coefficient (CTE) between Ag and ZnO induced thermal stresses in the silver which led to work hardening and an increase in the dislocation density of the metallic matrix [28, 29]. The work hardening of the matrix affects the mechanical properties of the composite and increases the properties such as hardness. Meanwhile, in case of ceramic matrix composites the induced thermal stresses might lead to

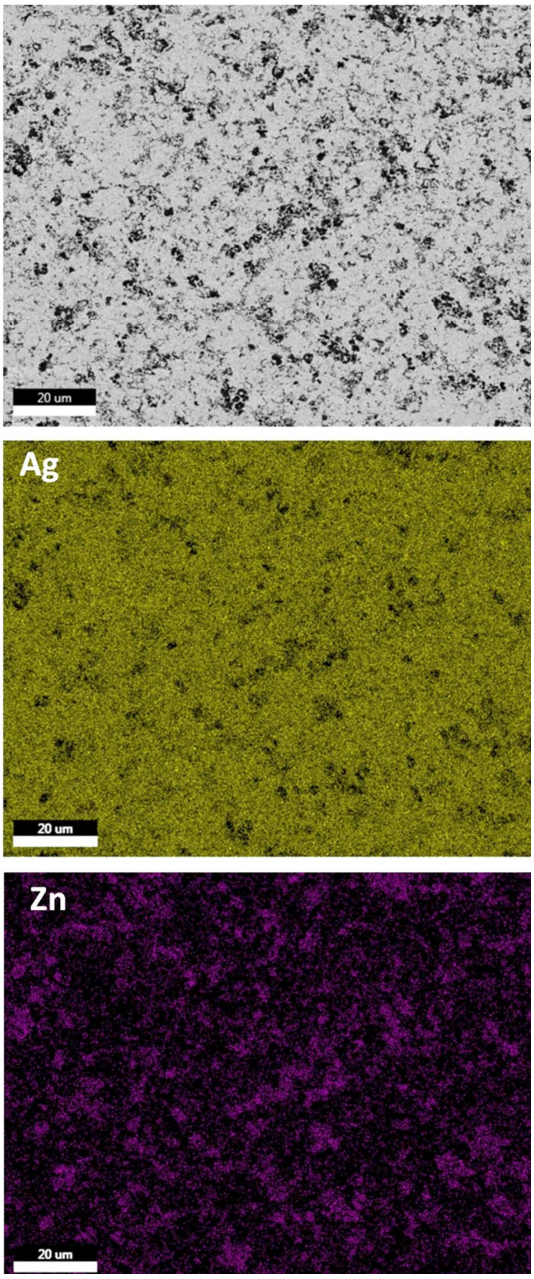

Fig. 7. Typical FESEM micrograph of the sintered samples with corresponding elemental map analysis of Ag and Zn.

crack formation within the matrix phase due to low ductility [30].

4. Conclusion

The present study aimed to synthesize Ag/ 8 wt.% ZnO composites, and the following results were

obtained:

1. Nearly dense and homogenous Ag/ZnO composites could be synthesized via co-precipitation and SPS methods.

2. The appropriate time for densification of the synthesized Ag/ZnO composite powders was about 5 min under 35 MPa in vacuum. Prolonging the sintering time to 10 min did not affect the densification and properties of the sintered samples.

3. The punch displacement versus temperature curve during the SPS process showed three distinct regions with different slopes which implied the change of the densification mechanisms by increasing the sintering temperature.

5. References

[1] H. Singh, G. Singh Brar, H. Kumar, V. Aggarwal, A review on metal matrix composite for automobile applications, *Materials Today: Proceedings*, 43(1) (2021) 320-325.

[2] K. K. Chawla, Composite Materials, Science and Engineering, Springer, New York, 2012, pp. 325-326.

[3] N. Chawla, K.K. Chawla, Metal Matrix Composites, Springer, New York, 2006, pp.239-243.

[4] T. X. Lu, C. G. Chen, Z. M. Guo, P. Li, M. X. Guo, Tungsten nanoparticle-strengthened copper composite prepared by a sol-gel method and in-situ reaction, *International Journal of Minerals, Metallurgy and Materials*, 26(11) (2019) 1477-1483.

[5] M. Ardestani, H. R. Rezaie, H. Arabi, H. Razavizadeh, The effect of sintering temperature on densification of nanoscale dispersed W–20–40wt.% Cu composite powders, *International Journal of Refractory Metals and Hard Materials*, 27(5) (2009) 862-867.

[6] M. Ardestani, Thermochemical synthesis and sintering of silver-8 wt.% copper oxide nanocomposite powders, *International Journal of Materials Research*, 106(12) (2015) 1294-1297.

[7] ASM International Handbook Committee, ASM Handbook Vol. 7 Powder Metallurgy, ASM International, Materials Park, Ohio, 2015, pp.790-798

[8] A. Pandey, P. Verma, O. P. Pandey, Comparison of properties of silver-tin oxide electrical contact materials through different processing routes, *Indian Journal of Engineering and Materials Science*, 15(3) (2008) 236-240.

[9] L. Münster, P. Bazant, M. Machovsky, I. Kuritka, Microwave-assisted hydrothermal synthesis of Ag/ZnO sub-microparticles, *Materiali in Tehnologije*, 49(2) (2015) 281-284.

[10] D.Guzman, C. Aguilar, P. Rojas, J. M. Criado, M. J. Dianez, R. Espinoza, A. Guzman, C. Martinez, Production of Ag−ZnO powders by hot mechanochemical processing, *Transactions of Nonferrous Metals Society of China*, 29(2) (2019) 365-373.

[11] P. B. Joshi, V. J. Rao, B. R. Rehani, Silver-zinc oxide electrical contact materials by mechanochemical synthesis route, *Indian Journal of Pure and Applied Physics*, 45(1) (2007) 9-15.

[12] F. S. Jazi, N. Parvin, M. R. Rabiei, M. R. Tahriri, Z. M. Shabestari, A. R. Azadmehr, The effect of the synthesis route on the grain size and morphology of ZnO/Ag nanocomposite, *Journal of Ceramic Processing Research*, 13(5) (2012) 523‑526.

[13] M. Ardestani, M. Zakeri, M. J. Nayyeri, M. R. Babollhavaejie, Synthesis of Ag–ZnO composites via ball milling and hot pressing processes, *Materials Science-Poland*, 32(1) (2014) 121-125.

[14] P. Cavaliere, Spark Plasma Sintering of Materials, Springer Nature, Switzerland, 2019, pp.3-20.

[15] Y. Wang, X. Ran, G. Barber, Q. Zou, Microstructure and sintering mechanism of C/Cu composites by mechanical alloying/spark plasma sintering, *Journal of Composite Mater*ials, 51(21) (2017) 3065-3074.

[16] A. Kokabi, M. Ardestani, M. Tamizifar, A. Abbasi, Characterization of TiO_2-reinforced bronze matrix composite prepared by SPS and PSR densification methods, *JOM*, 71(8) (2019) 2522-2530.

[17] Z. Branković, D. Luković-Golić, A. Radojković, J. Ćirković, D. Pajić, Z. Marinković-Stanojević, J. Xing, M. Radović, G. Li, G. Branković, Spark plasma sintering of hydrothermally synthesized bismuth ferrite, *Processing and Application of Ceramics*, 10(4) (2016) 257-264.

[18] N. Ray, B. Kempf, G. Wiehl, T. Mützel, F. Heringhaus, L. Froyen, K. Vanmeensel, J. Vleugels, Novel processing of Ag-WC electrical contact materials using spark plasma sintering, *Materials & Design*, 121 (2017) 262-271.

[19] H. Li, X. Wang, Y. Fei, H. Zhang, J. Liu, Z. Li, Y. Qiu, Effect of electric load characteristics on the arc erosion behavior of Ag-8wt.% Ni electrical contact material prepared by spark plasma sintering, *Sensors and Actuators A: Physical*, 326 (2021) 112718.

[20] M. Ghambari, T. Ebadzadeh, A. H. Pakseresht, E. Ghasali, Preparation of Ag/reduced graphene oxide reinforced copper matrix composites through spark plasma sintering: An investigation of microstructure and mechanical properties, *Ceramics International*, 46(9) (2020) 13569-13579.

[21] M. Ardestani, Chemical synthesis and densification behavior of Ag/ZnO metal matrix composite. *Materiali in Technologije*, 50(2) (2016) 281-286.

[22] W. D. Callister, D. G. Rethwisch, Materials Science and Engineering; An Introduction, John Wiley & Sons, Inc., USA, 2010, pp.523-525.

[23] R. M. German, Sintering from empirical observations to scientific principles, Elsevier, USA, 2014, pp.141-183.

[24] S. Diouf, A. Molinari, Densification mechanisms in spark plasma sintering: Effect of particle size and pressure, *Powder Technology*, 221 (2012) 220-227.

[25] S. Devaraj, S. Sankarany and R. Kumar, Influence of spark plasma sintering temperature on the densification, microstructure and mechanical properties of Al-4.5 wt.% Cu alloy, *Acta Metallurgica Sinica (English Letters)*, 26(6) (2013) 761-771.

[26] S. R. Oke, O. O. Ige, O. E. Falodun, B. A. Obadele, M. B. Shongwe, P. A. Olubambi, Optimization of process parameters for spark plasma sintering of nano structured SAF 2205 composite. *Journal of Materials Research and Technology*, 7(2) (2018) 126-134.

[27] Z. Y. Hu, Z. H. Zhang, X. W. Cheng, F. C. Wang, Y. F. Zhang, S. L. Li, A review of multi-physical fields induced phenomena and effects in spark plasma sintering: Fundamentals and applications, *Materials & Design*, 191 (2020) 108662.

[28] D. Dunand, A. Mortensen, Thermal mismatch dislocations produced by large particles in a strain-hardening matrix, *Materials Science and Engineering: A*, 135 (1991) 179-184.

[29] K. T. Kashyap, C. Ramachandra, C. Dutta, B. Chatterji, Role of work hardening characteristics of matrix alloys in the strengthening of metal matrix composites, *Bulletin of Materials Science*, 23(1) (2000) 47-49.

[30] K. K. Chawla, Ceramic Matrix Composites, Springer Science, New York, 2003, pp.106-138.